

## Optimization of thermochromic VO<sub>2</sub> based structures with tunable thermal emissivity

R. Li Voti, M. C. Larciprete, G. Leahu, C. Sibilìa, and M. Bertolotti

Citation: *J. Appl. Phys.* **112**, 034305 (2012); doi: 10.1063/1.4739489

View online: <http://dx.doi.org/10.1063/1.4739489>

View Table of Contents: <http://jap.aip.org/resource/1/JAPIAU/v112/i3>

Published by the [American Institute of Physics](http://www.aip.org).

---

### Related Articles

Asymmetric Fano resonance in eye-like microring system

*Appl. Phys. Lett.* **101**, 021110 (2012)

Simultaneous high-resolution two-dimensional spatial and one-dimensional picosecond streaked x-ray pinhole imaging

*Rev. Sci. Instrum.* **83**, 10E504 (2012)

Extraordinary optical transmission and extinction in a Terahertz wire-grid polarizer

*Appl. Phys. Lett.* **100**, 231912 (2012)

Note: A monolithic filter cavity for experiments in quantum optics

*Rev. Sci. Instrum.* **83**, 066101 (2012)

Quantitative scheme for full-field polarization rotating fluorescence microscopy using a liquid crystal variable retarder

*Rev. Sci. Instrum.* **83**, 053705 (2012)

---

### Additional information on J. Appl. Phys.


Journal Homepage: <http://jap.aip.org/>

Journal Information: [http://jap.aip.org/about/about\\_the\\_journal](http://jap.aip.org/about/about_the_journal)

Top downloads: [http://jap.aip.org/features/most\\_downloaded](http://jap.aip.org/features/most_downloaded)

Information for Authors: <http://jap.aip.org/authors>

## ADVERTISEMENT



**IBD Optical Film Quality at PVD Rates**

Advanced Optical Thin Films

Wide Range of Applications

Superior Throughput and Repeatability

**SPECTOR-HT ION BEAM DEPOSITION SYSTEMS**

**Veeco**

Innovation. Performance. Brilliant.

[www.veeco.com/spectorht](http://www.veeco.com/spectorht)

# Optimization of thermochromic VO<sub>2</sub> based structures with tunable thermal emissivity

R. Li Voti, M. C. Larciprete, G. Leahu, C. Sibilia, and M. Bertolotti

Department of Basic and Applied Science for Engineering, Sapienza Università di Roma, via A. Scarpa 16, 00161 Roma, Italy

(Received 3 April 2012; accepted 27 June 2012; published online 2 August 2012)

In this paper, we design and simulate VO<sub>2</sub>/metal multilayers to obtain a large tunability of the thermal emissivity of infrared (IR) filters in the typical mid wave IR window of many infrared cameras. The multilayer structure is optimized to realise a low emissivity filter at high temperatures useful for military purposes. The values of tunability found for VO<sub>2</sub>/metal multilayers are larger than the value for a single thick layer of VO<sub>2</sub>. © 2012 American Institute of Physics. [<http://dx.doi.org/10.1063/1.4739489>]

## I. INTRODUCTION

The term *infrared signature* generically describes how objects appear to infrared sensors. In most cases, infrared (IR) emissions from vehicles are used to detect, track, and lock-on to targets. The infrared signature of a given object depends on several factors, including the shape and size of the object, its temperature and its emissivity, as well as external conditions (illumination, background, to name some). One of the most challenging tasks regarding the IR vision is to reduce the infrared signature of objects.

Although the IR spectrum extends from red light to microwave radiation, i.e., 0.77–1000 μm, there are only two wavelength ranges showing high IR transmittance in the atmosphere, i.e., 3–5 and 8–12 μm, known as the mid wave IR (MWIR) and long wave IR (LWIR) windows, respectively. Outside these windows, CO<sub>2</sub> and H<sub>2</sub>O vapour give rise to both absorption and scattering phenomena, producing strong attenuation of IR radiation.

Thermochromic materials, changing their spectral properties as a function of the temperature, are extensively studied in the search for active control of thermal emission. These are, for example, niobium dioxide (NbO<sub>2</sub>), vanadium sesquioxide (V<sub>2</sub>O<sub>3</sub>), and vanadium dioxide (VO<sub>2</sub>). The most known and widely used is vanadium dioxide, VO<sub>2</sub>, that is also the object of the present study.<sup>1</sup> Its crystalline lattice exhibits an abrupt semiconductor-to-metal phase transition at a temperature  $T_C = 341$  K (68 °C), characterized by an increase of reflectivity as well as a decrease of emissivity in the IR range. On microscopic scales, the phase transition in VO<sub>2</sub> produces a physical change of its crystalline cell from monoclinic to tetragonal.

VO<sub>2</sub> shows insulating behavior below  $T_C$ , whereas above this temperature it exploits a metallic nature, dramatically changing its optical, electrical, and magnetic properties. In particular, the optical properties are sharply changed during the phase semiconductor-to-metal transition; thus, the dispersion law of the complex refractive index  $n + ik$  is strongly modified.<sup>2–4</sup> As a consequence, the phase transition, occurring during a very short temporal range of the order of few picoseconds, can be exploited for the realization of optical component switching from transparent (in the semiconductor state)

to reflective (in the metallic state), as well as for efficient thermal switches.<sup>5,6</sup>

In general, the performance of either optical or thermal switches can be quantified and estimated through the so-called *dynamic range*, which is the difference between the largest and smallest possible values of a changeable quantity. Within the present work, we define this figure of merit as the difference between the emissivity values, averaged in the IR range 3–5 μm and calculated for two different regimes, i.e., below and above  $T_C$ . Given this assumption, the *sign* of the dynamic range completely changes the filter behavior and thus determines the type of application. A thermochromic filter displaying *positive* dynamic range, i.e., an IR emissivity decreasing with increasing temperature, is suitable for IR signature reduction as well as for smart windows for thermal control.<sup>7</sup> On the other hand, a *negative* dynamic range is required for space applications and emissivity control of spacecraft.<sup>8</sup>

Recent experimental and theoretical works have shown that the thermal emissivity variation with temperature (and the dynamic range) of VO<sub>2</sub> thin films is strongly influenced by the substrate used for the deposition.<sup>9,10</sup>

In what follows, we consider simulations of the optical response of VO<sub>2</sub> thin films first deposited on different substrates (Sec. II), and then in multilayer structures (Sec. III), below and above the  $T_C$ . We discuss the effect that different substrates as well as VO<sub>2</sub> layer thicknesses have on the sign of the dynamic range. Finally, we introduce some metallo-dielectric multilayer structures, composed of alternating copper or silver and VO<sub>2</sub> layers, where the layer thickness is systematically varied in order to further increase and optimize the dynamic range.

## II. THERMAL EMISSIVITY AND INFRARED SIGNATURE FOR VO<sub>2</sub> THIN FILM

A study for the design and optimization of the VO<sub>2</sub> films may start from the calculation of the emissivity of VO<sub>2</sub> thin films on several different substrates with varying film thickness. As well known from Kirchhoff's law, the directional spectral emittance is equal to the directional spectral absorptance so that  $\varepsilon = 1 - R - T$ , where R and T, respectively, are the reflectance and transmittance of the structure.

To compare the different structures one fundamental quality factor to be introduced is the *tunability of emissivity* defined as the difference of the emissivity of the cold film minus the emissivity of the hot film. This quantity is usually averaged over the narrow window of the particular infrared camera [ $\lambda_{\min}$ ,  $\lambda_{\max}$ ] (in our example the MWIR window 3–5  $\mu\text{m}$ ) as follows:

$$\Delta\varepsilon_{av} = \frac{\int_{\lambda_{\min}}^{\lambda_{\max}} \Delta\varepsilon d\lambda}{\lambda_{\max} - \lambda_{\min}} = \frac{\int_{\lambda_{\min}}^{\lambda_{\max}} (\varepsilon_c - \varepsilon_h) d\lambda}{\lambda_{\max} - \lambda_{\min}}, \quad (1)$$

where  $\varepsilon_c$  and  $\varepsilon_h$  correspond, respectively, to the emissivity of the filter when *cold* or *hot* with respect to the transition temperature. Figure 1 shows the average tunability of the emissivity  $\Delta\varepsilon_{av}$  as a function of the vanadium dioxide thickness. The curves refer to different substrates with optical properties taken from the literature: infrared transparent substrates ( $\text{CaF}_2$ : blue curve.<sup>11</sup> Si: pink curve<sup>12</sup>), infrared opaque or metallic substrate (copper: black curve<sup>12,13</sup>), and as a reference, a hypothetical free standing  $\text{VO}_2$  film in air (red curve). The emissivity is here calculated as  $\varepsilon = 1 - R - T$  for normal incidence by using transfer matrix method. In the figure, the inset shows the behaviour at small  $\text{VO}_2$  thickness (micron).

The average tunability of emissivity might change sign on varying the vanadium dioxide thickness  $d_{\text{VO}_2}$ . For example, in the case of the  $\text{VO}_2/\text{CaF}_2$  system (blue curve), the average tunability reaches a minimum value of about  $\Delta\varepsilon_{av} = -0.4$  for  $d_{\text{VO}_2} = 20$  nm (thin layer), while for thick layers it changes sign giving  $\Delta\varepsilon_{av} > +0.3$  for  $d_{\text{VO}_2} = 20$   $\mu\text{m}$ . This behaviour is confirmed from the simulated emissivity spectra shown in Fig. 2. The emissivity of the sample with the thin  $\text{VO}_2$  layer (20 nm) increases with temperature (see dotted lines: blue for  $\varepsilon_c$ , red for  $\varepsilon_h$ ), while the opposite happens for the sample with the thick  $\text{VO}_2$  layer (20  $\mu\text{m}$ ) (see solid lines: blue for  $\varepsilon_c$ , red for  $\varepsilon_h$ ). In this last case, interference fringes also appear in both MWIR and LWIR (blue

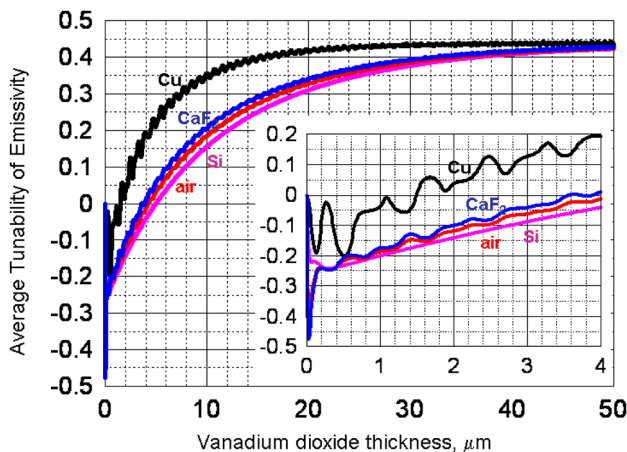


FIG. 1. Average tunability of emissivity vs the vanadium dioxide thickness for different substrates: copper (black line), silicon (pink line), calcium fluoride (blue line), and none (red line). Inset: magnification of the small vanadium dioxide thickness range.

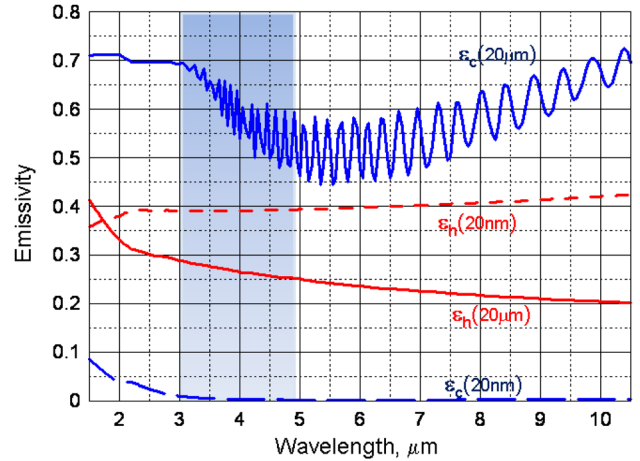


FIG. 2. *Cold* and *hot* emissivity spectra of  $\text{VO}_2/\text{CaF}_2$  for both thin and thick vanadium dioxide thicknesses. Cold 20  $\mu\text{m}$  layer (blue solid line); hot 20  $\mu\text{m}$  layer (red solid line); cold 20 nm layer (blue dotted line); hot 20 nm layer (red dotted line).

solid line). Their spacing is of the order of the wavelength, and the vanadium dioxide is in the semiconductor state.

In order to design an IR tunable filter, one must be able to reduce the infrared signature of hot objects; the requirement is to work with a structure with a large and positive tunability  $\Delta\varepsilon_{av} > 0$ . This is achieved by increasing the film thickness (see Fig. 1), and also by using metallic absorbing substrates able to enhance the whole *cold* emissivity  $\varepsilon_c$  when vanadium dioxide is in the semiconducting state. The black curve in Fig. 1, corresponding to a copper substrate, shows an enhancement of the tunability up to the limiting value of  $\Delta\varepsilon_{av} = +0.45$ . Similar behaviour is seen when using other metallic substrates.

We may now ask if it is possible to achieve a further enhancement of the tunability by using a more complex structure which uses vanadium dioxide and metal layers.

### III. SIGNATURE REDUCTION WITH AN OPTIMIZED $\text{VO}_2/\text{METAL}$ MULTILAYER

Here, we study how to enhance the tunability of a single  $\text{VO}_2$  film by designing an optimized  $\text{VO}_2/\text{metal}$  multilayer structure acting as a *tunable transparent metal*. Transparent metals basically are 1D photonic band gap (PBG) multilayers which exhibit passband properties in the optical range. This unusual and rare property of transparency for metals is achieved by growing an adequate sequence of metal thin layers ( $\approx 10$  nm) and transparent dielectric thick layers. Thanks to the tunnelling phenomena in the metal layers<sup>14–16</sup> and the interference effects in the dielectric layers,<sup>17</sup> these structures are able to enhance the transmittance at some wavelengths.

After some preliminary tests, we have chosen to optimise a structure of Fig. 3 which satisfies the following requirements:<sup>14,18</sup>

- It is made up of an odd number  $N$  of layers. A number of  $(N + 1)/2$   $\text{VO}_2$  layers are alternated with a number of  $(N - 1)/2$  metallic layers.
- The two outer vanadium dioxide layers have the same thickness  $d_{\text{extVO}_2}$ :

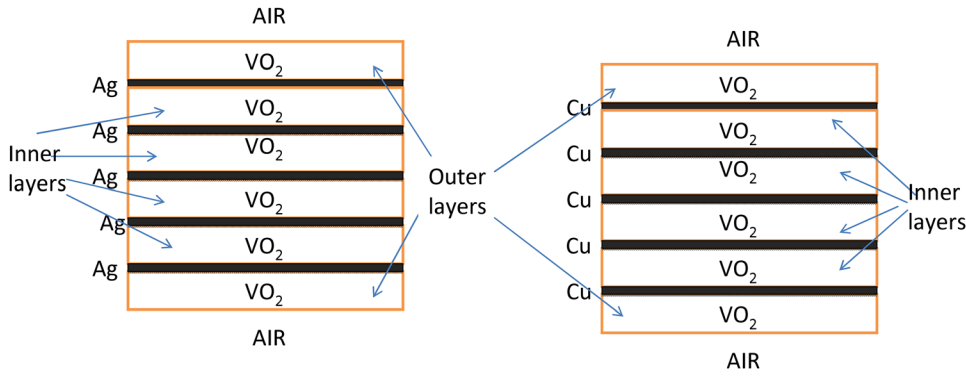


FIG. 3. Sketch of the  $\text{VO}_2/\text{Ag}$  and  $\text{VO}_2/\text{Cu}$  multilayers structures. The number of layers is here, for example,  $N = 7$ .

- (c) The inner vanadium dioxide layers have the same thickness  $d_{\text{intVO}_2}$ ;
- (d) Each metal layer (Cu or Ag) is 10 nm thick so to guarantee optical tunnelling.

Although this structure does not maximize the number of degrees of freedom (i.e., thicknesses of the different layers), it is sufficiently flexible. An example of an optimization is reported below for a  $\text{VO}_2/\text{Cu}$  structure made of  $N = 9$  layers. The 4 layers of Cu are 10 nm thick. Simulations were made by changing the vanadium dioxide thicknesses of both the inner layers of thickness  $d_{\text{intVO}_2}$  and outer layers of thickness  $d_{\text{extVO}_2}$  in the range of 0-500 nm. The tunability of the emissivity for each layer pair [ $d_{\text{intVO}_2}$ ,  $d_{\text{extVO}_2}$ ] is shown using a contour plot in Fig. 4(a). The maximum of  $\Delta\varepsilon_{\text{av}} = +0.53$  is reached when  $d_{\text{intVO}_2} = 370$  nm and  $d_{\text{extVO}_2} = 230$  nm. Some remarks immediately follow:

- (a) The value  $\Delta\varepsilon_{\text{av}} = +0.53$  is larger than the asymptotic limit of +0.45 of Fig. 1 obtained with a single thick layer of  $\text{VO}_2$ . This justifies the use of multilayered structures with thinner layers of  $\text{VO}_2$  and metal. Note that the total amount of vanadium dioxide is less than  $1.5 \mu\text{m}$ .
- (b) From the contours one may see that the choice of the optimal thicknesses  $d_{\text{intVO}_2}$  and  $d_{\text{extVO}_2}$  is not critical and allows relatively large tolerances (20 nm).
- (c) Since a quarter wavelength layer of thickness  $\lambda_o/4 n \approx 300$  nm for cold vanadium dioxide ( $<68^\circ\text{C}$ ) is appropriate at the central wavelength  $\lambda_o = 4 \mu\text{m}$  of the MWIR window, it appears that the optimized value  $d_{\text{intVO}_2} = 370$  nm follows the rules of quarter wavelength stacks normally used in antireflection structures. This implies that the optimization procedure converges towards structures with minimum reflection (at  $T < 68^\circ\text{C}$ ) so to maximize the absorbance (i.e., emissivity) in the metal layers. This is clear in Figs. 5 and 6. One can see that the quantity  $\Delta\varepsilon_{\text{av}}$  is also maximized.

The second example in Fig. 4(b) shows the optimization for the same  $\text{VO}_2/\text{Cu}$  structure but with a very large number of layers ( $N = 21$ ) in order to check if any asymptotic limit for the obtainable value of  $\Delta\varepsilon_{\text{av}}$  exists. The maximum of the average emissivity is now  $\Delta\varepsilon_{\text{av}} = +0.67$  for  $d_{\text{intVO}_2} = 420$  nm and  $d_{\text{extVO}_2} = 230$  nm. As  $N$  increases there is an increase of  $\Delta\varepsilon_{\text{av}}$  and an adjustment of  $d_{\text{intVO}_2}$  which finally stabilizes to 420 nm.

The emissivity spectra of the  $\text{VO}_2/\text{Cu}$  optimized structures are shown in Fig. 5(a). As the number of layers increases (the arrow shows the sequence  $N = 9, 11, 13, 15, 17$ ) the *cold* emissivity spectra  $\varepsilon_c$  also increases, tending to 1 (maximum emissivity) in the MWIR window, whereas the *hot* emissivity spectra  $\varepsilon_h$  are practically unchanged because the IR emission comes entirely from the surface  $\text{VO}_2$  layer that becomes a thick metallic layer for  $T > 68^\circ\text{C}$ . Fig. 5(b) is the same as Fig. 5(a) with silver substituting copper.

The reasons for the large *cold* emissivity  $\varepsilon_c$  in the MWIR window are clearly put into evidence in Fig. 6 where

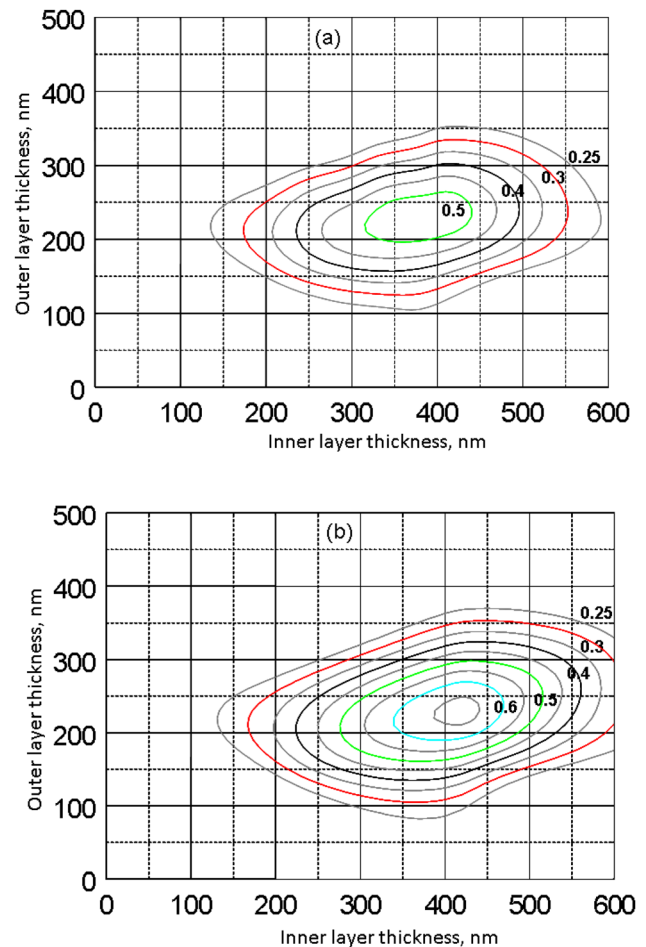


FIG. 4. Contour plot of the average tunability of emissivity of  $\text{VO}_2/\text{Cu}$  multilayer as a function of the inner  $\text{VO}_2$  layer thickness  $d_{\text{intVO}_2}$  and outer  $\text{VO}_2$  layer thickness  $d_{\text{extVO}_2}$  as introduced in Fig. 3: (a) multilayered structure with  $N = 9$  made of a total thickness of 40 nm of copper and (b) multilayered structure with  $N = 21$  made of a total thickness of 100 nm of copper.

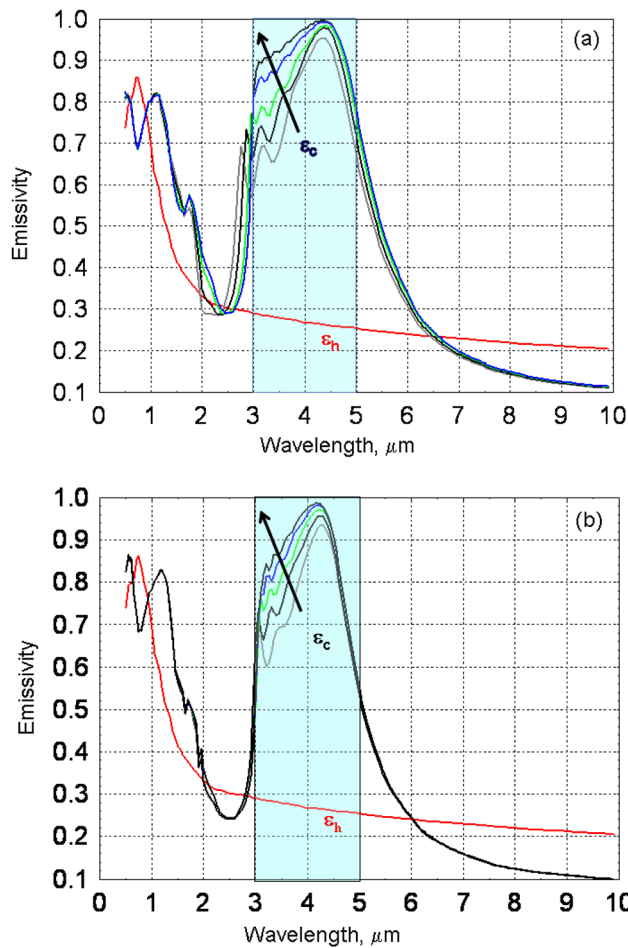


FIG. 5. Cold and hot emissivity spectra for VO<sub>2</sub>/metal optimized multilayers: (a) emissivity vs wavelength for VO<sub>2</sub>/Cu optimized multilayers. Hot emissivity  $\epsilon_h$  at temperature  $T > 68^\circ\text{C}$  (red curve). Cold emissivity  $\epsilon_c$  for multilayers with an increasing number of layers  $N = 9, 11, 13, 15, 17$  (other colors) and (b) emissivity vs wavelength for VO<sub>2</sub>/Ag optimized multilayers. Hot emissivity  $\epsilon_h$  at temperature  $T > 68^\circ\text{C}$  (red curve). Cold emissivity  $\epsilon_c$  for multilayers with an increasing number of layers  $N = 9, 11, 13, 15, 17$  (other colors).

both the reflectance (a) and transmittance (b) spectra are shown for the same VO<sub>2</sub>/Cu optimized multilayers discussed in Fig. 5(a). As expected Fig. 6(a) shows that for  $T < 68^\circ\text{C}$  these multilayers behave as antireflection nanostructures in the MWIR window; the reflectance curves  $R_c$  tend to 0 (thus maximizing  $\epsilon = 1 - R - T$ ) with slow or imperceptible improvement as  $N$  increases. On the other hand, Fig. 6(b) shows that the cold transmittance  $T_c$  decreases with the number of layers. Since the optimization procedure tends to maximize  $\epsilon_c = 1 - R_c - T_c$ , this is obtained by simply increasing  $N$  (the arrow shows the sequence  $N = 9, 11, 13, 15, 17$ ), so to increase the total amount of copper that can absorb light and consequently affect the emissivity.

The emissivity spectra for VO<sub>2</sub>/Ag-based structures are shown in Fig. 5(b); the arrow shows the sequence  $N = 9, 11, 13, 15, 17$ . In this case, the structures are optimized asymptotically with  $d_{\text{intVO}_2} = 430\text{ nm}$  and  $d_{\text{extVO}_2} = 240\text{ nm}$  but are less efficient than the VO<sub>2</sub>/Cu-based ones when considering the value of  $\Delta\epsilon_{\text{av}}$ . The reason can be understood from a comparison between Figs. 5(a) and 5(b). The emissivity spectra for cold VO<sub>2</sub>/Ag are narrow with respect to cold VO<sub>2</sub>/Cu and do not fit completely the MWIR window.

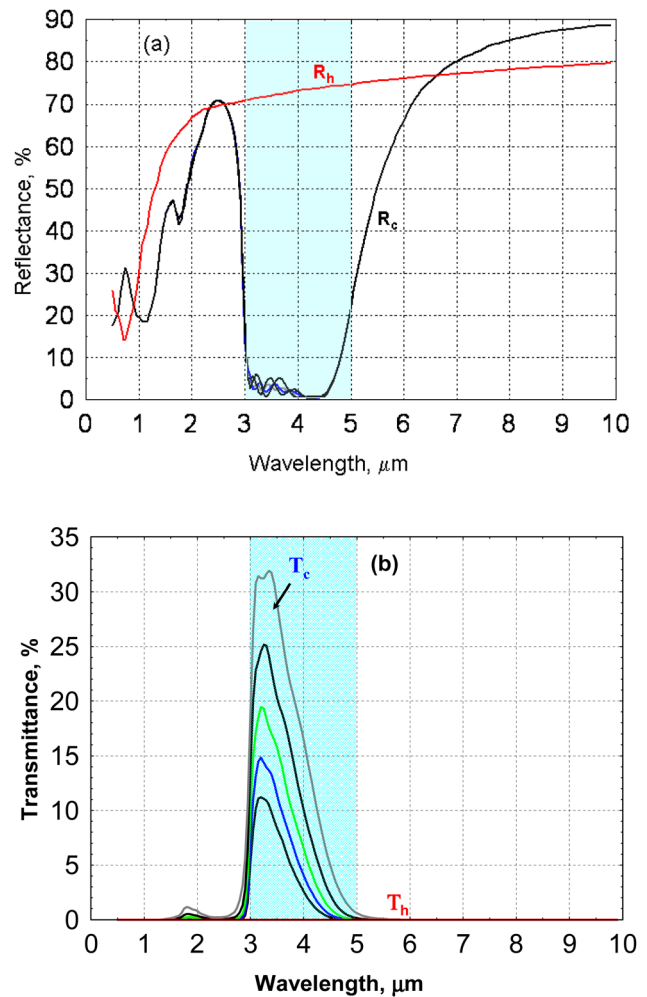


FIG. 6. Cold and hot reflectance and transmittance spectra for VO<sub>2</sub>/Cu optimized multilayers: (a) Reflectance vs wavelength; hot reflectance  $R_h$  at temperature  $> 68^\circ\text{C}$  (red curve); cold reflectance  $R_c$  for multilayers with an increasing number of layers  $N = 9, 11, 13, 15, 17$  (other colors). The curves are here undistinguishable. (b) Transmittance vs wavelength; hot transmittance  $T_h$  at temperature  $> 68^\circ\text{C}$  (red curve); cold transmittance  $T_c$  for multilayers with an increasing number of layers  $N = 9, 11, 13, 15, 17$  (other colors).

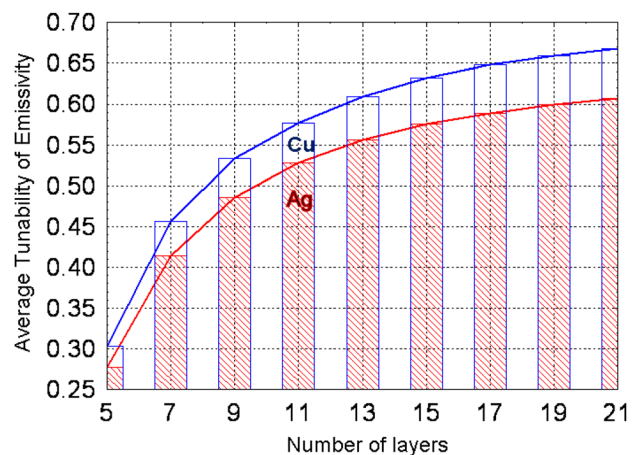


FIG. 7. Maximum tunability of emissivity obtained with optimized multilayers VO<sub>2</sub>/Ag based, and VO<sub>2</sub>/Cu based as a function of the number of layers  $N$ . Each metal layer is 10 nm thick.

These slight differences can quantitatively be shown in the average tunability of the emissivity as a function of  $N$  for the optimized VO<sub>2</sub>/Ag- and VO<sub>2</sub>/Cu-based multilayers as reported in Fig. 7. Whatever the number of layers  $N$ , copper shows better results.

Further enhancement of the tunability can be in principle obtained by using a 3D-VO<sub>2</sub> based photonic bandgap. Preliminary results are shown in Ref. 19.

#### IV. CONCLUSIONS

The results presented show the possibility of affecting the emissivity properties of VO<sub>2</sub> layers with temperature by playing with a number of different parameters, i.e., the layer thickness, the substrate material, and the use of multilayer structures. The temporal response of the thermal transition is affected by all these parameters and should be investigated in future experiments.

#### ACKNOWLEDGMENTS

This work has been performed in the framework of the contract “FISEDA” granted by Italian Ministry of Defence. The authors are grateful to O. B. Wright for useful discussions.

<sup>1</sup>M. M. Qazilbash, M. Brehm, B.-G. Chae, P.-C. Ho, G. O. Andreev, B.-J. Kim, S. J. Yun, A. V. Balatsky, M. B. Maple, F. Keilmann, H.-T. Kim, and D. N. Basov, *Science* **318**, 1750 (2007).

<sup>2</sup>H. Kakiuhida, P. Jin, S. Nakao, and M. Tazawa, *Jpn. J. Appl. Phys., Part 1* **46**, 113 (2007).

<sup>3</sup>G. Guzman, F. Beteille, R. Morineau, and J. Livage, *J. Mater. Chem.* **6**, 505 (1996).

<sup>4</sup>O. P. Konovalova, A. I. Sidorov, and I. I. Shagonov, *J. Opt. Technol.* **66**, 391 (1999).

<sup>5</sup>A. B. Pevtsov, D. A. Kurdyukov, V. G. Golubev, A. V. Akimov, A. A. Meluchev, A. V. Sel'kin, A. A. Kaplyanskii, D. R. Yakovlev, and M. Bayer, *Phys. Rev. B* **75**, 153101 (2007).

<sup>6</sup>V. G. Golubev, V. Yu. Davydov, N. F. Kartenko, D. A. Kurdyukov, A. V. Medvedev, A. B. Pevtsov, A. V. Scherbakov, and E. B. Shadrin, *Appl. Phys. Lett.* **79**, 2127 (2001).

<sup>7</sup>F. Guinneton, L. Sauques, J.-C. Valmatette, F. Cros, and J.-R. Gavarr, *Thin Solid Films* **446**, 287 (2004).

<sup>8</sup>M. Benkahoul, M. Chaker, J. Margot, E. Haddad, R. Kruzelecky, B. Wong, W. Jamroz, and P. Poinas, *Sol. Energy Mater. Sol. Cells* **95**, 3504 (2011).

<sup>9</sup>H. S. Choi, J. S. Ahn, J. H. Jung, T. W. Noh, and D. H. Kim, *Phys. Rev. B* **54**, 4621 (1996).

<sup>10</sup>R. O. Dillon, K. Le, and N. Ianno, *Thin Solid Films* **398–399**, 10 (2001).

<sup>11</sup>I. H. Malitson, *Appl. Opt.* **2**, 1103 (1963).

<sup>12</sup>*Handbook of Optical Constants of Solids*, edited by E. D. Palik (Academic, New York, 1985).

<sup>13</sup>C. L. Foiles, “Optical properties of pure metals and binary alloys,” *Landolt and Bornstein, Group III: Condensed Matter: Electronic Properties-Metals: Electronic Transport Phenomena-Electrical Resistivity, Thermoelectrical Power and Optical Properties* (Springer Verlag, 1985), Vol. 15b.

<sup>14</sup>M. S. Sarto, R. Li Voti, F. Sarto, and M. C. Larciprete, *IEEE Trans. Electromagn. Compat.* **47**, 602 (2005).

<sup>15</sup>M. C. Larciprete, C. Sibilìa, S. Paoloni, M. Bertolotti, F. Sarto, and M. Scalora, *J. Appl. Phys.* **93**, 5013 (2003).

<sup>16</sup>M. Scalora, M. J. Bloemer, A. S. Manka, S. D. Pethel, J. P. Dowling, and C. M. Bowden, *J. Appl. Phys.* **83**, 2377 (1998).

<sup>17</sup>M. C. Larciprete, C. Sibilìa, S. Paoloni, G. Leahu, R. Li Voti, M. Bertolotti, M. Scalora, and K. Panajotov, *J. Appl. Phys.* **92**, 2251 (2002).

<sup>18</sup>R. Li Voti, *Rom. Rep. Phys.* **64**(2), 446–466 (2012). Available via [http://www.rp.infm.ro/2012\\_64\\_2.html](http://www.rp.infm.ro/2012_64_2.html).

<sup>19</sup>G. Leahu, R. Li Voti, C. Sibilìa, M. Bertolotti, V. Golubev, and D. A. Kurdyukov, *Opt. Quantum Electron.* **39**, 305 (2007).